JITK (JURNAL ILMU PENGETAHUAN DAN TEKNOLOGI KOMPUTER)

VOL. 12. NO. 2 NOVEMBER 2026
P-ISSN: 2685-8223 | E-ISSN: 2527-4864
DOI: 10.33480/jitk.v12i2.8558

LINEAR, NON-LINEAR AND EDGE-PRESERVING FILTERS FOR GAUSSIAN NOISE REDUCTION IN BRAIN MRI: A COMPARISON

Eka Wahyu Hidayat[1*], Euis Nur Fitriani Dewi[1], Dhea Nurlita[1]

Universitas Siliwangi, Tasikmalaya, Indonesia[1]
www.unsil.ac.id[1]
ekawahyu@unsil.ac.id[*], euis.nurfitriani@unsil.ac.id, dheanurlitasa23@gmail.com

(*) Corresponding Author
(Responsible for the Quality of Paper Content)

The creation is distributed under the Creative Commons Attribution-NonCommercial 4.0 International License

Submitted: 02 June 2026, **Revised:** 11 November 2026, **Accepted:** 17 November 2026, **Published:** 20 November 2026.

Abstract— *This study presents a controlled baseline evaluation of Gaussian Filter, Median Filter, and Bilateral Filter for reducing Gaussian noise in brain MRI images. The study aims to provide a reproducible preprocessing benchmark rather than propose a new denoising algorithm. A total of 376 JPG-format brain MRI images from the AD MRI Dataset for Stage Classification were resized to 128×128 pixels and contaminated with zero-mean Gaussian noise with a variance of 0.01. The noisy images were processed using Gaussian Filter with a 5×5 kernel and σ = 1, Median Filter with a 5×5 kernel, and Bilateral Filter with σs = 2 and σr = 25. Performance was evaluated using PSNR, SSIM, MSE, benefit-cost Min-Max normalization, and Euclidean Distance-based ranking. The results confirm that Gaussian Filter achieved the lowest mean Euclidean Distance of 0.920399911, followed by Median Filter at 0.971186494 and Bilateral Filter at 0.989926281. Gaussian Filter also produced the best result on 241 of 376 images and obtained the lowest mean Euclidean Distance across all MRI classes. These findings show that the expected compatibility between Gaussian noise and Gaussian-based smoothing was consistently reflected under the tested condition. Therefore, this study provides a transparent baseline reference for MRI image preprocessing before applying more complex denoising models. Further validation using DICOM/NIfTI data, multiple noise conditions, parameter optimization, and paired statistical testing is required.*

Keywords: *Bilateral filter, gaussian filter, image denoising, median filter, MRI.*

INTRODUCTION

Magnetic Resonance Imaging (MRI) is widely used for observing brain structures because it provides strong soft-tissue contrast and enables detailed visualization of anatomical information compared with several other imaging modalities such as CT scans, PET scans, and X-rays [3]. However, MRI images may experience quality degradation during acquisition and processing due to noise. One type of noise commonly used to simulate image degradation is Gaussian noise, which can obscure anatomical details, reduce contrast, and decrease the visibility of tissue structures in medical images [2]. Such degradation may be caused by electronic interference, thermal fluctuations, acquisition device limitations, and imaging conditions that reduce the signal-to-noise ratio [3]. Therefore, noise reduction is an important preprocessing stage in MRI image processing because improved image quality can support visual interpretation and subsequent computational analysis.

Various methods have been developed to reduce noise in medical images, ranging from conventional filtering techniques to deep learning-based approaches. A theoretical review of denoising techniques for brain MRI and lung HRCT images has been conducted [4]; however, it did not specifically include direct testing on a brain MRI image dataset using a standardized quantitative evaluation framework. Other studies have applied Gaussian Filter, Median Filter, and Bilateral Filter to non-medical images, such as general digital images and tomato leaf images [5], [6]. Although these studies remain relevant as references for fundamental

denoising techniques, their findings cannot be directly generalized to brain MRI images because MRI data have distinct intensity patterns, tissue structures, and sensitivity to subtle detail variations.

Several comparative studies have evaluated conventional filtering methods, but their scope remains limited for the context of MRI denoising. A comparison between Median Filter and Gaussian Filter has been conducted on images contaminated with salt-and-pepper noise [7]. However, that study did not include Bilateral Filter, even though this method has edge-preserving capability and can reduce noise while maintaining edge information. In addition, Gaussian Filter, Median Filter, and Bilateral Filter have been compared on general digital images [8], but the evaluation was not specifically directed toward brain MRI images. These conditions indicate that a direct and controlled comparison of the three filters on MRI images remains necessary.

Recent MRI denoising studies have increasingly focused on more complex noise modeling techniques, including native noise modeling and deep learning-based approaches. Ssentamu et al. introduced a native noise denoising approach for low-field MRI images by utilizing the intrinsic noise characteristics of MRI acquisition data, indicating that MRI noise characteristics may differ from those represented by simple synthetic noise simulations [2]. In addition, Deng et al. developed a sparse mixture-of-experts approach for reducing non-uniform noise in MRI images, demonstrating that modern MRI denoising research is increasingly moving toward adaptive and deep learning-based methods [9]. Nevertheless, conventional filtering methods remain important as baseline approaches because they are simple, computationally efficient, easy to implement, and interpretable. Therefore, evaluating fundamental methods such as Gaussian Filter, Median Filter, and Bilateral Filter remains relevant for establishing baseline performance in MRI image preprocessing.

Gaussian Filter, Median Filter, and Bilateral Filter were selected in this study because they represent three different filtering characteristics. Gaussian Filter is a linear smoothing filter that performs pixel intensity smoothing based on a Gaussian distribution, making it relevant for reducing Gaussian noise when appropriate sigma (σ) values and kernel sizes are selected [10], [11], [12]. Median Filter is a non-linear order-statistic filter that replaces each pixel value with the median value of its neighboring pixels and is widely used for reducing noise while preserving certain image details [13]. In MRI images, Median Filter has also been reported to be effective in handling impulsive noise, producing favorable PSNR values while preserving image edges at low-to-moderate noise levels [14]. Meanwhile, Bilateral Filter is an edge-preserving filter that considers both spatial proximity and pixel intensity similarity, allowing it to reduce noise while maintaining image edge details. Based on these characteristics, the three methods represent linear, non-linear, and edge-preserving filtering approaches, respectively [15].

Despite the availability of conventional and learning-based MRI denoising methods, the role of classical filters as transparent baselines remains relevant. Their performance is not determined by the filter category alone; it also depends on the assumed noise model, image intensity scale, parameter configuration, and the image structures that must be preserved. Comparisons conducted on general-purpose images or under impulse-noise conditions do not necessarily establish the relative behaviour of these filters on brain MRI images. Moreover, a method that reduces pixelwise error may not preserve local structural information to the same extent. This motivates an evaluation that reports complementary error-based and structure-based measures rather than relying on a single metric.

This study therefore conducts a controlled baseline comparison of Gaussian, median, and bilateral filtering on a labelled subset of brain MRI images contaminated with a specified synthetic additive Gaussian-noise condition. The contribution is methodological and empirical, not algorithmic: (1) the three filters are applied to identical noisy inputs; (2) the image intensity scale, noise-generation procedure, and filter parameters are explicitly documented; (3) parameter sensitivity is examined so that the comparison is not interpreted solely from one arbitrary parameter setting; and (4) pixelwise and structural quality measures are reported separately, with any aggregate ranking justified and accompanied by metric-level results [16], [17], [18], [19], [20]. The findings are limited to the dataset format, preprocessing pipeline, and noise conditions evaluated here and are intended as a reproducible reference for subsequent experiments, not as evidence of clinical denoising performance.

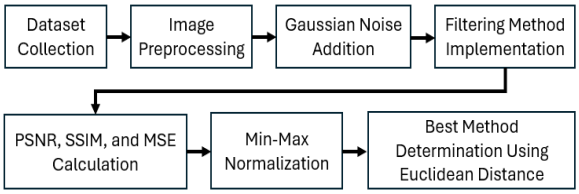
MATERIALS AND METHODS

This study employs an experimental approach to compare the performance of Gaussian Filter, Median Filter, and Bilateral Filter in reducing Gaussian noise in MRI images. The research process was conducted systematically to ensure that each

Accredited Rank 2 (SINTA 2) based on Decree No. 225/E/KPT/2022 issued by Direktorat Jenderal Pendidikan Tinggi, Riset, dan Teknologi, Kementerian Pendidikan, Kebudayaan, Riset, dan Teknologi Republik Indonesia, dated December 7, 2022. Published by LPPM Universitas Nusa Mandiri.

VOL. 12. NO. 2 NOVEMBER 2026
P-ISSN: 2685-8223 | E-ISSN: 2527-4864
DOI: 10.33480/jitk.v12i2.8558

method was tested under the same conditions, allowing the comparison results to be objective and reproducible. The research stages include dataset collection, image preprocessing, noise addition, filtering method implementation, evaluation metric calculation, value normalization, and determination of the best-performing method using Euclidean Distance. The general research workflow is illustrated in Figure 1.



Source: (Research Results, 2026)

Figure 1. Research Stages

Dataset Collection

The dataset was obtained from the AD MRI Dataset for Stage Classification distributed through Kaggle and described by its source as derived from the Alzheimer's Disease Neuroimaging Initiative (ADNI). The analysed subset contained 376 JPG images assigned to four dataset labels: NonDemented (ND), VeryMildDemented (VMD), MildDemented (MD), and ModerateDemented (MoD). Each class contained 94 images (Table 1). Images were selected through random sampling without replacement from each class. No random seed was explicitly specified during the sampling process, and no additional screening for duplicate or corrupted images was performed. The dataset labels were retained as dataset categories and were not independently verified as clinical diagnoses.

All source images were provided in JPG format and resized to 128 × 128 pixels using the default bicubic interpolation method of MATLAB's imresize() function. The resizing process was applied consistently to all images to standardize their spatial dimensions before noise generation and filtering. However, JPG compression and image resizing may alter fine anatomical structures and intensity distributions. Therefore, the present study evaluates the performance of denoising methods on preprocessed digital MRI images rather than raw clinical MRI acquisitions. Consequently, the findings should not be interpreted as clinical validation.

Image Preprocessing

Images were read using MATLAB's imread() function, converted to grayscale where applicable, and resized to 128 × 128 pixels using the default bicubic interpolation method of imresize(). The source images were represented as 8-bit unsigned integers (uint8), with a nominal intensity range of [0, 255]. The same reference image was retained for all filtering method comparisons. No additional contrast enhancement was applied. The preprocessing procedure was implemented using MATLAB R2025b to facilitate experimental reproducibility.

Noise Model and Parameter Setting

Before noise generation, each grayscale image was represented using JPEG (uint8) with an intensity range of [0, 255]. The additive noise was generated in this intensity domain; consequently, the noise variance and bilateral range parameter are interpreted relative to this same scale. The noisy realization for each image was held constant across the three filtering methods to ensure paired inputs. The comparative experiments were conducted using fixed parameter configurations for each filtering method. Specifically, the Gaussian filter employed a 5 × 5 kernel with a standard deviation (σ) of 1, the median filter used a 5 × 5 neighbourhood, and the bilateral filter used a spatial standard deviation (σs) of 2 and a range standard deviation (σr) of 25.

These parameter values were established as predefined experimental settings and were consistently applied across all test images to ensure uniform evaluation conditions. No parameter optimization or sensitivity analysis was performed in this study. The bilateral range parameter σr controls the influence of intensity similarity and must be expressed in the same units as the image intensities. Therefore, its numerical value depends on the image intensity representation, whether [0, 1] or [0, 255].

Method Implementation

The experiment was implemented in MATLAB R2025b through a Graphical User Interface (GUI). For each image, the processing pipeline comprised: (1) reading the JPG file using imread(); (2) grayscale conversion, where applicable, and resizing to 128 × 128 pixels using the default bicubic interpolation of imresize(); (3) generating additive Gaussian noise using imnoise(I, 'gaussian', 0, 0.01); (4) applying Gaussian, Median, and Bilateral filters to the same noisy image; and (5) calculating and recording the evaluation metrics, including PSNR, SSIM, and MSE. The Gaussian noise was generated with zero mean and a variance of 0.01 on MATLAB's normalized intensity scale [0, 1]. No random seed was explicitly specified. The imnoise() function constrains the output intensities to the valid range of the image data type. All filtering methods were evaluated using fixed parameter

CC BY NC

configurations to maintain consistent experimental conditions.

Experimental Data Recording

For each of the 376 images, three filtered outputs were produced, resulting in 1,128 processed images. The evaluation values of PSNR, SSIM, and MSE were recorded for each method and each image. The results were tabulated in Microsoft Excel and grouped by class to support both overall and class-wise performance analysis.

Analysis and Evaluation

Image quality was evaluated using PSNR, SSIM, and MSE. PSNR and MSE quantify pixelwise reconstruction error, whereas SSIM assesses similarity in luminance, contrast, and local structure. Because PSNR is a logarithmic transformation of MSE when the peak intensity is fixed, the two measures are mathematically dependent. To avoid counting essentially the same error information twice, MSE is reported as a supplementary descriptive measure and is not included in the primary composite ranking. For the composite analysis, PSNR and SSIM were converted to benefit-oriented values and combined using an equal-weight Euclidean distance to the ideal point. Let p_{ij} and s_{ij} denote the PSNR and SSIM values for method j on image i. The normalized values are defined as:

$$p'_{ij} = (p_{i,j} - p_{min})/(p_{max} - p_{min}) \quad (1)$$

$$s'_{ij} = (s_{i,j} - s_{min})/(s_{max} - s_{min}) \quad (2)$$

where p_min and p_max are the minimum and maximum PSNR values, and s_min and s_max are the corresponding SSIM bounds, calculated across all three filtering methods and all 376 test images (1,128 method–image observations). The distance to the ideal point (1,1) is:

$$d_{ij} = \sqrt{\{\frac{\left[\left(1-p'_{ij}\right)^2+\left(1-s'_{ij}\right)^2\right]}{2}\}} \quad (3)$$

Equal weighting in Equation (3) is used as a transparent descriptive choice because no externally validated preference weights are available. This score is not a clinical utility function. Since Min–Max normalization is data-dependent, the bounds and comparison set are reported, and the resulting ranking is interpreted only within this experiment. PSNR, SSIM, and MSE are also presented individually so that the composite score does not conceal metric-specific trade-offs. PSNR was used to determine the quality of the filtered image compared with the original image. A higher PSNR value indicates better image quality because the remaining noise or error is lower. The PSNR formula is presented in Equation (4), as adopted from [21], [22].

$$PSNR = 10 \times log_{10}\left(\frac{MAX_I^2}{MSE}\right) \quad (4)$$

In Equation (4), MAX_I represents the maximum pixel intensity value of the image. For an 8-bit image, the value of MAX_I is 255, while MSE represents the mean squared error between the original image and the filtered image. MSE is used to calculate the average squared difference between the pixels of the original image and those of the filtered image. A lower MSE value indicates a smaller difference between the filtered image and the original image, suggesting better noise reduction performance. The MSE formula is presented in Equation (5), as adopted from [22]

$$MSE(x,y) = \frac{1}{MN}\sum_{i=1}^{M}\sum_{j=1}^{N}[x(i,j) - y(i,j)]^2 \quad (5)$$

In Equation (5), $x(i,j)$ represents the pixel value of the original image at position (i,j), while $y(i,j)$ represents the pixel value of the filtered image at the same position. Meanwhile, (M) and (N) indicate the image dimensions, corresponding to the number of rows and columns, respectively. In addition to PSNR and MSE, the evaluation was also performed using SSIM to measure the similarity between the original image and the filtered image based on visual image characteristics. SSIM considers three main components: luminance, contrast, and structure. The SSIM value ranges from 0 to 1, where a value closer to 1 indicates a higher level of similarity between the filtered image and the original image. The SSIM formula is presented in Equation (6), as adopted from [22].

$$SSIM(x,y) = \frac{(2\mu_x\mu_y+C_1)(2\sigma_{xy}+C_2)}{(\mu_x^2+\mu_y^2+C_1)(\sigma_x^2+\sigma_y^2+C_2)} \quad (6)$$

In Equation (6), μ_x and μ_y represent the mean intensity values of images x and y, Meanwhile, σ_x^2 and σ_y^2 denote the variances of images x and y, while σ_{xy} represents the covariance between the two images. The constants C_1 and C_2 are used to

Accredited Rank 2 (SINTA 2) based on Decree No. 225/E/KPT/2022 issued by Direktorat Jenderal Pendidikan Tinggi, Riset, dan Teknologi, Kementerian Pendidikan, Kebudayaan, Riset, dan Teknologi Republik Indonesia, dated December 7, 2022. Published by LPPM Universitas Nusa Mandiri.

VOL. 12. NO. 2 NOVEMBER 2026
P-ISSN: 2685-8223 | E-ISSN: 2527-4864
DOI: 10.33480/jitk.v12i2.8558

prevent division by zero during the calculation process. Since PSNR, SSIM, and MSE have different value ranges, a normalization process is required so that the three metrics can be compared on the same scale. Normalization was performed using the Min-Max Normalization method to transform each metric value into a range between 0 and 1. The normalization formula is presented in Equation (7), as adopted from [22].

$$x' = \frac{x - x_{min}}{x_{max} - x_{min}} \quad (7)$$

In Equation (7), x represents the original value of a metric, x_{min} denotes the minimum value, x_{max} denotes the maximum value, and x' represents the normalized value. However, because MSE has different characteristics from PSNR and SSIM, its normalization procedure must be treated differently. PSNR and SSIM are considered benefit criteria because higher values indicate better image quality. In contrast, MSE is considered a cost criterion because lower values indicate better image quality. Therefore, the normalized MSE value must be transformed into a benefit-oriented value using Equation (8).

$$MSE'_{benefit} = 1 - \frac{MSE - MSE_{min}}{MSE_{max} - MSE_{min}} \quad (8)$$

Equation (8) is used to ensure that the normalized MSE value has the same direction of interpretation as PSNR and SSIM. Therefore, after normalization, values closer to 1 indicate better performance for all evaluation metrics. Once all metrics are represented on the same scale, the next stage is to determine the best-performing filtering method using Euclidean Distance. This calculation measures the distance between the normalized metric values and the ideal point. The ideal point used in this study is (1,1,1), which represents the best possible condition: high PSNR, high SSIM, and low MSE after transformation into a benefit-oriented criterion. The Euclidean Distance formula is presented in Equation (9), as adopted from [22].

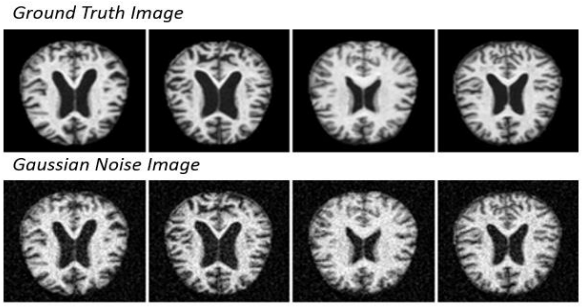
$$d = \sqrt{(1 - x_1)^2 + (1 - x_2)^2 + (1 - x_3)^2} \quad (9)$$

In Equation (9), (d) represents the Euclidean Distance value, while x_1, x_2, x_3 denote the normalized values of PSNR, SSIM, and MSE, respectively. A smaller Euclidean Distance value indicates that the filtering result is closer to the ideal condition. Therefore, the method with the smallest Euclidean Distance value is considered the best-performing method for reducing Gaussian noise in MRI images.

RESULTS AND DISCUSSION

Data Preparation and Noise Adding

The experiment began with the collection and selection of 376 brain MRI images using a random sampling method. These images were used as reference images (*ground truth*) for the method comparison process. All images were standardized to a resolution of 128×128 pixels in JPG format; therefore, no additional preprocessing was required apart from data consistency verification. Representative ground-truth images used in this study are illustrated in the upper section of Figure 2. Subsequently, Gaussian noise with a variance of 0.01 was added to each ground-truth image to produce noise-contaminated images, as illustrated in the lower part of Figure 2. The addition of synthetic noise was intended to simulate image degradation that may occur in MRI images, allowing the noise reduction performance of Gaussian Filter, Median Filter, and Bilateral Filter to be evaluated under controlled conditions and compared objectively based on the selected evaluation metrics.



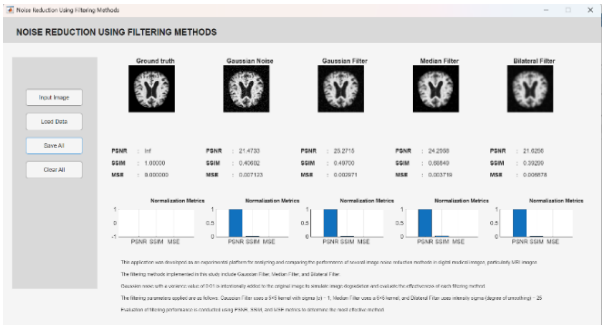
Source: (Research Results, 2026)
Figure 1. Ground Truth and Gaussian Noise Image

Method Implementation

The methods were implemented using a MATLAB R2025b-based application equipped with a Graphical User Interface (GUI). The application was developed to facilitate the implementation of the filtering algorithms and the systematic evaluation of their noise reduction performance on brain MRI images. All input images were resized to a resolution of 128 × 128 pixels. To establish a consistent experimental condition, zero-mean Gaussian noise with a variance of 0.01 was added to each image before the filtering process. The application subsequently processed the noisy images using the three filtering methods and calculated their respective performance metrics for

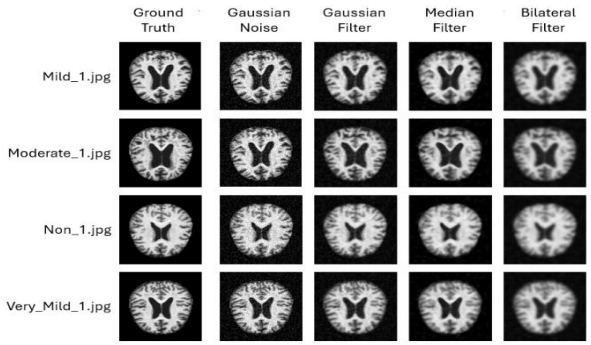
CC BY NC

comparative evaluation. The application interface used in the testing process is shown in Figure 3.



Source: (Research Results, 2026)
Figure 3. Application Interface for Testing Process

The application generates noise-reduced output images using Gaussian Filter, Median Filter, and Bilateral Filter, and displays the normalized PSNR, SSIM, and MSE values. The results are visualized through image comparisons and bar charts to support both visual and quantitative analysis. Representative testing results are shown in Figure 4, comparing the ground-truth images, Gaussian noise-contaminated images, and filtered outputs from each method.



Source: (Research Results, 2026)
Figure 4. Test Results on Sample Images

After testing all 376 MRI images, evaluation data for PSNR, SSIM, and MSE were obtained. All processed images were stored in the "*Hasil_Noise_Reduction*" folder, which contains the ground-truth images, noise-contaminated images, Gaussian Filter outputs as detailed in Table 1, Median Filter outputs as shown in Table 2, and Bilateral Filter outputs as presented in Table 3. Evaluation results for each method in Excel format.

Table 1. Gaussian Filter Test Result

No	Images	Gaussian Filter		
		PSNR	SSIM	MSE
1	Mild_1	25,2715	0,497	0,002971
2	Moderate_1	25,0604	0,49319	0,003119
3	Non_1	25,8502	0,49485	0,0026
4	Verymild_1	24,963	0,48833	0,003189
...	...	...	...	...
376	Verymild_94	25,219	0,472	0,00301

Source: (Research Results, 2026)

Table 2. Median Filter Test Result

No	Images	Median Filter		
		PSNR	SSIM	MSE
1	Mild_1	24,2958	0,68849	0,003719
2	Moderate_1	23,7197	0,67773	0,004247
3	Non_1	25,0879	0,68889	0,003099
4	Verymild_1	23,5756	0,66401	0,00439
...	...	...	...	...
376	Verymild_94	24,239	0,6519	0,00377

Source: (Research Results, 2026)

Table 3. Bilateral Filter Test Result

No	Images	Bilateral Filter		
		PSNR	SSIM	MSE
1	Mild_1	21,6256	0,39299	0,006878
2	Moderate_1	21,229	0,3766	0,007535
3	Non_1	22,6298	0,40443	0,005458
4	Verymild_1	21,4976	0,37397	0,007083
...	...	...	...	...
376	Verymild_94	22,314	0,3714	0,00587

Source: (Research Results, 2026)

Value Normalization

The PSNR, SSIM, and MSE metrics have different value ranges, requiring Min-Max Normalization to standardize their values between 0 and 1 for fair comparison. PSNR and SSIM were classified as benefit criteria, where higher values indicate better image quality, while MSE was treated as a cost criterion, where lower values indicate smaller reconstruction errors. The normalized results for the Gaussian, Median, and Bilateral filters are presented in Tables 4, 5, and 6, respectively.

Table 4. Gaussian Filter Normalization Results

No	Images	Gaussian Filter		
		PSNR	SSIM	MSE
1	Mild_1	0,50061	0,9315	0,457537
2	Moderate_1	0,49646	0,4014	0,478873
3	Non_1	0,57563	0,7978	0,365854
4	Verymild_1	0,13209	0,7536	0,838462
...	...	...	...	...
376	Verymild_94	0,25417	0,3599	0,7

Source: (Research Results, 2026)

Table 5. Median Filter Normalization Results

No	Images	Median Filter		
		PSNR	SSIM	MSE
1	Mild_1	0,45864	0,96057	0,48218
2	Moderate_1	0,46244	0,57920	0,49359
3	Non_1	0,48338	0,87387	0,41935
4	Verymild_1	0,10268	0,47732	0,85447
...	...	...	...	...
376	Verymild_94	0,288192	0,21598	0,62313

Source: (Research Results, 2026)

Accredited Rank 2 (SINTA 2) based on Decree No. 225/E/KPT/2022 issued by Direktorat Jenderal Pendidikan Tinggi, Riset, dan Teknologi, Kementerian Pendidikan, Kebudayaan, Riset, dan Teknologi Republik Indonesia, dated December 7, 2022. Published by LPPM Universitas Nusa Mandiri.

VOL. 12. NO. 2 NOVEMBER 2026
P-ISSN: 2685-8223 | E-ISSN: 2527-4864
DOI: 10.33480/jitk.v12i2.8558

Table 6. Bilateral Filter Normalization Results

No	Images	Bilateral Filter		
		PNSR	SSIM	MSE
1	Mild_1	0,296492	0,8393	0,6470
2	Moderate_1	0,242138	0,2050	0,7261
3	Non_1	0,413511	0,9407	0,4949
4	Verymild_1	0,167098	0,3582	0,7649
...	...	...	...	...
376	Verymild_94	0,378168	0,2805	0,5154

Source: (Research Results, 2026)

Method Performance Comparison

After normalization, Euclidean Distance (ED) was calculated for each image and each filtering method. Since Gaussian Filter, Median Filter, and Bilateral Filter were applied to the same 376 MRI images, the comparison was treated as a paired measurement. Therefore, in addition to descriptive statistics, a paired statistical significance test was performed to strengthen the interpretation of method performance.

The overall ED performance is presented in Table 7. Gaussian Filter obtained the lowest mean ED value of 0.920399911, followed by Median Filter at 0.971186494 and Bilateral Filter at 0.989926281. Gaussian Filter also produced the highest number of best results, achieving the lowest ED on 241 out of 376 images, while Median Filter and Bilateral Filter achieved the best results on 63 and 72 images, respectively. These results indicate that Gaussian Filter was descriptively the closest method to the ideal normalized condition under the tested Gaussian noise scenario.

Table 7. Euclidean Distance Performance by Filter

Method	Gaussian Filter	Median Filter	Bilateral Filter
Mean Euclidean Distance	0.920399911	0.97118 6494	0.9899262 81
Standard Deviation	0.1241103 67	0,13517 6708	0.1308487 45
Median	0,8963761 19	0,94521 1793	0.9694985 04
Interquartile Range	0.1653829 62	0.19518 6538	0.1914353 53
95% Confidence Interval	0.9078549 24 – 0.9329448 98	0,95752 2929 – 0.98485 0059	0.9767001 84 – 1.0031523 78
Best Result	241	63	72

Source: (Research Results, 2026)

To determine whether the observed differences were statistically significant, the Friedman test was applied because three related filtering methods were evaluated on the same image set. The Friedman test indicated a statistically significant overall difference among the three filtering methods, $\chi^2(2) = 126.574$, $p < 0.001$, with Kendall's W = 0.168 indicating a relatively small effect magnitude. Pairwise post-hoc comparisons were conducted using the Wilcoxon signed-rank test, with Holm adjustment for the three comparisons. All Holm-adjusted p-values were below 0.001. Paired effect sizes were not available from the reported results. Statistical significance was interpreted alongside the observed performance differences rather than as evidence of practical or clinical superiority. The analysis treated each image as one paired observation. As participant identifiers were unavailable, potential correlations among images originating from the same participant could not be assessed. Consequently, image-level statistical tests may overestimate the effective sample size, and this limitation should be considered when interpreting the findings.

Class-wise performance is presented in Table 8 to examine whether the method ranking was consistent across different MRI image categories. Gaussian Filter obtained the lowest mean ED in all four classes, namely ND, VMD, MD, and MoD. This indicates that Gaussian Filter provided the most consistent performance across the evaluated MRI classes. However, the difference between Gaussian Filter and Bilateral Filter in the MD class was relatively small, suggesting that class-specific image characteristics may influence the relative performance of filtering methods.

Table 8. Class-wise Euclidean Distance Performance

Class	Gaussian Mean ± SD	Median Mean ± SD	Bilateral Mean ± SD	Best Method
ND	0.935010149 ± 0.109429582	1.005473732 ± 0.136735757	1.016334093 ± 0.129683437	Gaussian Filter
VMD	0.885451590 ± 0.097299702	0.960069861 ± 0.117493896	0.999720700 ± 0.122511730	Gaussian Filter
MD	0.955335174 ± 0.137437325	0.960782233 ± 0.139009750	0.955678142 ± 0.133360585	Gaussian Filter
MoD	0.892111756 ± 0.146872977	0.936363784 ± 0.139526385	0.974677547 ± 0.131018433	Gaussian Filter

Source: (Research Results, 2026)

Analysis and Evaluation of Filtering

Based on the Euclidean Distance measurement results presented in Table 7 and Table 8, each filtering method showed different performance levels in reducing Gaussian noise in MRI images. Euclidean Distance was used to measure the proximity of the filtered images to the original images based on the combined normalized values of PSNR, SSIM, and MSE. A smaller Euclidean

CC BY NC

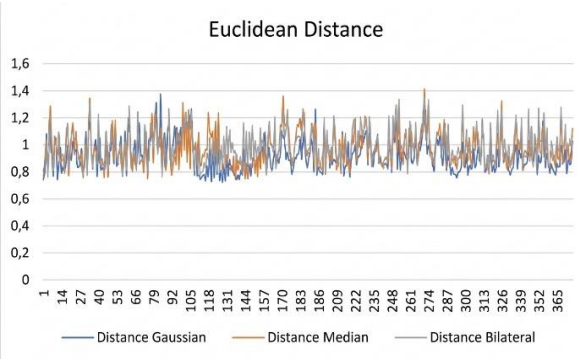
Distance value indicates better filtering performance because the filtered image is closer to the ideal normalized condition.

As shown in Table 7, Gaussian Filter achieved the lowest mean Euclidean Distance value of 0.920399911 with a standard deviation of 0.124110367. Its 95% confidence interval, ranging from 0.907854924 to 0.932944898, was also lower than those of Median Filter and Bilateral Filter. In addition, Gaussian Filter produced the best result on 241 out of 376 MRI images, indicating that it was not only superior in average performance but also more frequently generated the closest result to the original image.

Median Filter obtained a mean Euclidean Distance value of 0.971186494 with a standard deviation of 0.135176708, while Bilateral Filter obtained 0.989926281 with a standard deviation of 0.130848745. Although both methods were able to reduce noise, their average ED values were higher than that of Gaussian Filter. Median Filter generally performs better for impulse or salt-and-pepper noise, whereas this study used Gaussian noise. Meanwhile, Bilateral Filter, despite its edge-preserving capability, is highly influenced by the spatial sigma parameter (σs) and intensity sigma parameter (σr), which may affect the balance between noise reduction and edge preservation.

The class-wise evaluation in Table 8 further supports the overall results. Gaussian Filter achieved the lowest mean Euclidean Distance in all four MRI classes: ND, VMD, MD, and MoD. The obtained values were 0.935010149 ± 0.109429582 for ND, 0.885451590 ± 0.097299702 for VMD, 0.955335174 ± 0.137437325 for MD, and 0.892111756 ± 0.146872977 for MoD. Although the performance difference between Gaussian Filter and Bilateral Filter in the MD class was relatively small, Gaussian Filter still showed the lowest mean ED value. These results indicate that Gaussian Filter provided the most consistent performance across the evaluated MRI image classes.

The superior performance of Gaussian Filter can be attributed to the compatibility between its Gaussian-based smoothing mechanism and the Gaussian noise introduced in this study. However, this finding applies specifically to the tested conditions, namely JPG-format MRI images with a resolution of 128×128 pixels, Gaussian noise with a variance of 0.01, and fixed filter parameter configurations. Therefore, further evaluation using different noise levels, parameter variations, and original medical image formats such as DICOM or NIfTI is required to confirm the generalizability of the findings. The performance comparison of the three filtering methods is illustrated in Figure 5.



Source: (Research Results, 2026)

Figure 5. Comparison Results Chart

Discussion

The results indicate that Gaussian Filter achieved the best overall performance compared with Median Filter and Bilateral Filter based on Euclidean Distance values derived from PSNR, SSIM, and MSE. This finding is consistent with the Gaussian noise model employed in this study, as Gaussian smoothing effectively reduces random intensity variations. However, its smoothing mechanism may also suppress fine anatomical details, indicating a trade-off between noise reduction and structural preservation.

Median Filter demonstrated acceptable performance but was less effective than Gaussian Filter under the tested conditions. This outcome may be attributed to its greater suitability for impulse noise, such as salt-and-pepper noise, rather than Gaussian noise. Meanwhile, Bilateral Filter, despite its edge-preserving characteristics, did not achieve the best overall performance. Its effectiveness depends on the spatial (σs) and range (σr) parameters, which may influence the balance between noise suppression and structural preservation. Since fixed parameters were applied, the results do not establish the optimal performance achievable by either method.

Overall, the findings demonstrate that denoising performance depends on noise characteristics, image properties, and filter configurations. Under the experimental conditions involving 128 × 128 JPG-format MRI images, Gaussian noise with a variance of 0.01, and fixed filtering parameters, Gaussian Filter achieved the lowest Euclidean Distance. Nevertheless, this result reflects the evaluated image-processing conditions rather than evidence of clinical superiority.

The paired statistical comparisons support differences among the filtering methods within the evaluated dataset and experimental conditions but do not establish broader generalizability. Future research should investigate original DICOM or NIfTI images, more realistic noise models and noise

Accredited Rank 2 (SINTA 2) based on Decree No. 225/E/KPT/2022 issued by Direktorat Jenderal Pendidikan Tinggi, Riset, dan Teknologi, Kementerian Pendidikan, Kebudayaan, Riset, dan Teknologi Republik Indonesia, dated December 7, 2022. Published by LPPM Universitas Nusa Mandiri.

VOL. 12. NO. 2 NOVEMBER 2026
P-ISSN: 2685-8223 | E-ISSN: 2527-4864
DOI: 10.33480/jitk.v12i2.8558

levels, and independently optimized filtering parameters to assess the robustness and applicability of these findings.

CONCLUSION

This study compared Gaussian Filter, Median Filter, and Bilateral Filter as controlled baseline methods for reducing Gaussian noise in brain MRI images. The experiment used 376 JPG-format MRI images resized to 128×128 pixels, contaminated with Gaussian noise at a variance of 0.01, and evaluated using PSNR, SSIM, MSE, benefit-cost Min-Max normalization, and Euclidean Distance-based ranking. The results show that Gaussian Filter achieved the lowest mean Euclidean Distance value of 0.920399911, followed by Median Filter at 0.971186494 and Bilateral Filter at 0.989926281. Gaussian Filter also produced the highest number of best results, outperforming the other methods on 241 out of 376 images, and achieved the lowest mean Euclidean Distance across all evaluated MRI classes: ND, VMD, MD, and MoD. These findings confirm that, under a controlled Gaussian noise scenario, Gaussian-based smoothing provides the most consistent baseline performance compared with median-based and edge-preserving filtering.

The main implication of this study is that Gaussian Filter can serve as a simple and reproducible reference method for MRI image preprocessing under synthetic Gaussian noise conditions. However, this result should not be interpreted as evidence that Gaussian Filter is universally superior for all MRI denoising tasks. The use of compressed JPG images, a single synthetic noise condition, and fixed filter parameters means that the findings are most appropriate as a preprocessing baseline, not as a clinical or optimized denoising conclusion. Future studies should extend this baseline by using original DICOM or NIfTI data, evaluating more realistic noise variations, optimizing filter parameters, applying paired statistical testing, and comparing classical filters with adaptive and deep learning-based denoising models. The present statistical comparisons quantify differences within this dataset and experimental condition. Future studies should focus on external validation using raw MRI data, more realistic noise models, and parameter optimization rather than treating the current results as universally generalizable.

DECLARATION OF AI USE

The authors declare that ChatGPT (OpenAI) was used to assist with English language editing, grammar improvement, and manuscript clarity. All AI-assisted content was carefully reviewed and revised by the authors, who take full responsibility for the accuracy, originality, and final content of the manuscript.

AUTHOR CONTRIBUTIONS

This journal uses the Contributor Roles Taxonomy (CRediT) to identify individual author contributions to the research and manuscript preparation.

Author	Contribution Roles
Eka Wahyu Hidayat	Conceptualization, Supervision (Lead), Writing – Review & Editing.
Euis Nur Fitriani Dewi	Supervision (Supporting), Validation, Writing – Review & Editing.
Dhea Nurlita	Software, Writing – Original Draft.

ACKNOWLEDGMENTS

The authors would like to acknowledge the Multimedia and Game Technology Research Laboratory, Universitas Siliwangi, for providing the computer facilities used in this research. This study received no external funding, as it was conducted in part as an undergraduate student's final project.

FUNDING

This research received no specific grant from any funding agency in the public, commercial, or not-for-profit sectors.

CONFLICT OF INTEREST STATEMENT

The authors declare that there are no conflicts of interest related to the research, writing, or publication of this article.

REFERENCE

[1] Z. Akram, M. Faraz, U. Fatima, S. Zameer, Z. Anwar, Shamsuddin, S. Habib, M. Mustafa, "Role of CT Scan and MRI In Cancer Diagnosis: A Comparative Review Of Imaging Modalities For Precision Medicine," *J. Cancer Tumor Int.*, vol. 15, no. 3, pp. 179–189, Jul. 2025, doi: 10.9734/Jcti/2025/ V15i3312.

[2] P. S. E. Siagian, E. Y. Puspaningrum, W. S. W. Awang, I. G. S. M. Diyasa, "MRI Image Enhancement Of The Brain Using U-Net," *Simantec,* vol. 13, no. 2, pp. 125–136, 2023, doi: 10.21107/simantec.v13i2.29775.

[3] T. Ssentamu, A. Kimbowa, R. Omoding, E. Atamba, P. K. Mukwaya, G. W. Jjuuko,

CC BY NC

"Denoising Very Low-field Magnetic Resonance Images using Native Noise Modeling," *Frontiers in Neuroimaging*, vol. 4, 1501801, 2025, doi: 10.3389/fnimg.2025.1501801.

[4] A. Saini, A. Dogra, B. Goyal, V. Kukreja, "A Review and Experimental Analysis Of Denoising Techniques For Medical Images", *The Open Neuroimaging Journal*, vol. 18, 2025, doi: 10.2174/0118744400404813250924064413.

[5] D. Salsabilla, R. Wahyusari, "Perbandingan Metode Reduksi Noise Pada Citra Digital Berbasis Website," *J. Komtika Komputasi Dan Inform.*, vol. 9, no. 2, pp. 195–204, Nov. 2025, Doi: 10.31603/Komtika.V9i2.14966.

[6] A. Nabila, L. F. Iskandar. N. R. N. S. Lubis, Z. A. Gunawan, P. Hendri, E. P. Giri, G. P. Mindara, "Perbandingan Metode Filtering Untuk Peningkatan Kualitas Citra Daun Tomat Terinfeksi TMV," *J. Ilmu Komput. Dan Multimed.*, vol. 2, no. 2, pp. 1–6, Des. 2025, doi: 10.46510/Ilkomedia.V2i2.80.

[7] P. S. Alhirani, L. S. Harahap, R. Chantika, "Analisis Perbandingan Filter Median dan Gaussian dalam Mengurangi Noise pada Citra Digital," *J. Ilm. Tek. Inform. Dan Komun.*, vol. 5, no. 2, pp. 495–505, Jun. 2025, doi: 10.55606/Juitik.V5i2.1148.

[8] K. L. Lew, C. Y. Kew, K. S. Sim, S. C. Tan, "Adaptive Gaussian Wiener Filter For CT-Scan Images With Gaussian Noise Variance," *J. Inform. Web Eng.*, vol. 3, no. 1, pp. 169–181, Feb. 2024, doi: 10.33093/Jiwe.2024.3.1.11.

[9] Z. Deng, J. Campbell, "Sparse Mixture-of-Experts for Non-Uniform Noise Reduction in MRI Images," *Proceedings of the IEEE/CVF Winter Conference on Applications of Computer Vision Workshops*, 2025, doi: 10.1109/WACVW65960.2025.00036

[10] R. Szeliski, "Computer Vision: Algorithms And Applications", Springer. 2nd Edition.

[11] M. M. Weli, O. M. Abdullah, "Digital Image Noise Reduction Based on Proposed Smoothing And Sharpening Filters," *Indones. J. Comput. Sci.*, vol. 13, no. 4, Jul. 2024, doi: 10.33022/Ijcs.V13i4.4151.

[12] M. F. Alamsyah, L. S. Harahap, M. Firjatullah, "Meningkatkan Kualitas Gambar Digital Melalui Pengurangan Noise Menggunakan Median Filtering," *Data Sci. Indones. Dsi*, vol. 5, no. 1, pp. 96–104, Jul. 2025, doi: 10.47709/Dsi.V5i1.6290.

[13] C. Sabrine, S. Abir, "Median Filter For Denoising Mri," *Rev. Intell. Artif.*, vol. 36, no. 3, pp. 483–488, Jun 2022, doi: 10.18280/Ria.360317.

[14] S. M. A. Sharif, R. A. Naqvi, M. Biswas, W. K. Loh, "Deep Perceptual Enhancement For Medical Image Analysis," *Ieee J. Biomed. Health Inform.*, vol. 26, no. 10, pp. 4826–4836, Okt. 2022, doi: 10.1109/Jbhi.2022.3168604.

[15] A. Breger, A. Biguri, M. S. Landman, I. Selby, N. Amberg, E. Brunner, J. Gröhl, S. Hatamikia, C. Karner, L. Ning, S. Dittmer, M. Roberts, "A Study Of Why We Need To Reassess Full Reference Image Quality Assessment With Medical Images," *J. Imaging Inform. Med.*, vol. 38, no. 6, pp. 3444–3469, Mar. 2025, doi: 10.1007/S10278-025-01462-1.

[16] R. Wibisono, H. Soetanto, "Perbandingan Efektifitas Filter Median, Gaussian Dan Mean Dalam Mengurangi Noise Pada Citra Digital," *Semin. Nas. Mhs. Fak. Teknol. Inf. Senafti*, Sep. 2024.

[17] M. Dohmen, M. A. Klemens, I. M. Baltruschat, T. Truong, M. Lenga, "Similarity And Quality Metrics for MR Image-To-Image Translation," *Sci. Rep.*, vol. 15, no. 1, pp. 3853, Jan. 2025, doi: 10.1038/S41598-025-87358-0.

[18] M. Tsaqofah, L. Harahap, D. S. Hasibuan, "Optimization Of Digital Image Processing Through Gaussian Filtering For Noise Reduction," *J. Artif. Intell. Eng. Appl.*, vol. 4, pp. 1–5, Jun. 2025, doi:10.59934/jaiea.v4i3.1120

[19] F. Ullah, K. Kumar, T. Rahim, J. Khan, Y. Jung, "A New Hybrid Image Denoising Algorithm using Adaptive and Modified Decision-Based Filters for Enhanced Image Quality," *Sci. Rep.*, vol. 15, no. 1, pp. 8971, Mar. 2025, doi: 10.1038/S41598-025-92283-3.

[20] H. M. S. S. Herath, H. M. K. K. M. B. Herath, N. Madusanka, B. I. Lee, "A Systematic Review Of Medical Image Quality Assessment," *J. Imaging*, vol. 11, no. 4, pp. 100, Mar. 2025, doi: 10.3390/Jimaging11040100.

[21] Y. A. Najjar, "Comparative Analysis Of Image Quality Assessment Metrics: MSE, PSNR, SSIM and FSIM," *Int. J. Sci. Res. Ijsr*, vol. 13, no. 3, pp. 110–114, Mar. 2024, doi: 10.21275/Sr24302013533.

[22] S. Sinsomboonthong, B. N. Mandal, "Performance Comparison Of New Adjusted Min-Max With Decimal Scaling and Statistical Column Normalization Methods for Artificial Neural Network Classification," *Int. J. Math. Math. Sci.*, vol. 2022, pp. 1–9, Apr. 2022, doi: 10.1155/2022/3584406.

Accredited Rank 2 (SINTA 2) based on Decree No. 225/E/KPT/2022 issued by Direktorat Jenderal Pendidikan Tinggi, Riset, dan Teknologi, Kementerian Pendidikan, Kebudayaan, Riset, dan Teknologi Republik Indonesia, dated December 7, 2022. Published by LPPM Universitas Nusa Mandiri.